iTRAQ-based quantitative proteome analysis reveals metabolic changes between a cleistogamous wheat mutant and its wild-type wheat

Caiguo Tang [Equal first author, 1, 2], **Huilan Zhang** [Equal first author, 1, 2], **Pingping Zhang** [3], **Yuhan Ma** [1], **Minghui Cao** [1, 2], **Hao Hu** [1, 2], **Faheem Afzal Shah** [1], **Weiwei Zhao** [1], **Minghao Li** [Corresp., 1, 2], **Lifang Wu** [Corresp. 1]

[1] Key laboratory of high magnetic field and Ion beam physical biology, Hefei Institutes of Physical Science, Chinese Academy of Sciences, Hefei, Anhui, China

[2] School of Life Sciences, University of Science and Technology of China, Hefei, Anhui, China

[3] School of Life Sciences, Anhui University, Hefei, Anhui, China

Corresponding Authors: Minghao Li, Lifang Wu
Email address: limh@ipp.ac.cn, lfwu@ipp.ac.cn

Background: Wheat is one of the most important staple crops worldwide. *Fusarium* head blight severely affects wheat yield and quality. A novel bread wheat mutant, *ZK001*, characterised as cleistogamic was isolated from a non-cleistogamous variety (YM18) through static magnetic field mutagenesis. Cleistogamy is a promising strategy for controlling *Fusarium* head blight. However, little is known about the mechanism of cleistogamy in wheat. **Methods:** We performed a *Fusarium* head blight resistance test to identify the *Fusarium* head blight infection rate of *ZK001*. We also measured the agronomic traits of *ZK001* and the starch and total soluble sugar contents of lodicules in YM18 and *ZK001*. Finally, we performed comparative studies at the proteome level between YM18 and *ZK001* based on the proteomic technique of isobaric tags for relative and absolute quantification. **Results:** The infection rate of *ZK001* was lower than that of its wild type and AK58. The abnormal lodicules of *ZK001* lost the ability to push the lemma and palea apart during the flowering stage. Proteome analysis showed that the main differentially abundant proteins were related to carbohydrate metabolism, protein transport, and calcium ion binding. These differentially abundant proteins may work together to regulate cellular homeostasis, osmotic pressure and the development of lodicules. This theory is supported by the analysis of starch, soluble sugar content in the lodicules as well as the results of qRT-PCR. **Conclusions:** In this paper, we demonstrate that proteome analysis provides comprehensive information that will be useful for further research on the lodicule development mechanism in wheat. The *ZK001* mutant is optimal for studying flower development in wheat and could be very important for *Fusarium* head blight resistant projects via conventional crossing.

iTRAQ-based quantitative proteome analysis reveals metabolic changes between a cleistogamous wheat mutant and its wild-type wheat

Caiguo Tang [1,2,†], Huilan Zhang [1,2,†], Pingping Zhang [3], Yuhan Ma [1], Minghui Cao [1,2], Hao Hu [1,2], Faheem Afzal Shah [1], Weiwei Zhao [1], Minghao Li [1,2,*] and Lifang Wu [1,*]

[1] Key laboratory of high magnetic field and Ion beam physical biology, Hefei Institutes of Physical Science, Chinese Academy of Sciences, Hefei, Anhui, China;
[2] School of Life Sciences, University of Science and Technology of China, Hefei, Anhui, China
[3] School of Life Sciences, Anhui University, Hefei, Anhui, China

[†] These authors contributed equally to this work.
*Corresponding Author:
Minghao Li; Lifang Wu
350 Shushanhu Road, Hefei 230031, Anhui, P. R. China
Email address: limh@ipp.ac.cn (M.L); lfwu@ipp.ac.cn (L.W)

Abstract

Background: Wheat is one of the most important staple crops worldwide. *Fusarium* head blight severely affects wheat yield and quality. A novel bread wheat mutant, *ZK001*, characterised as cleistogamic was isolated from a non-cleistogamous variety (YM18) through static magnetic field mutagenesis. Cleistogamy is a promising strategy for controlling *Fusarium* head blight. However, little is known about the mechanism of cleistogamy in wheat.
Methods: We performed a *Fusarium* head blight resistance test to identify the *Fusarium* head blight infection rate of *ZK001*. We also measured the agronomic traits of *ZK001* and the starch and total soluble sugar contents of lodicules in YM18 and *ZK001*. Finally, we performed comparative studies at the proteome level between YM18 and *ZK001* based on the proteomic technique of isobaric tags for relative and absolute quantification.
Results: The infection rate of *ZK001* was lower than that of its wild type and AK58. The abnormal lodicules of *ZK001* lost the ability to push the lemma and palea apart during the flowering stage. Proteome analysis showed that the main differentially abundant proteins were related to carbohydrate metabolism, protein transport, and calcium ion binding. These differentially abundant proteins may work together to regulate cellular homeostasis, osmotic pressure and the development of lodicules. This theory is supported by the analysis of starch, soluble sugar content in the lodicules as well as the results of qRT-PCR.

Conclusions: In this paper, we demonstrate that proteome analysis provides comprehensive information that will be useful for further research on the lodicule development mechanism in wheat. The *ZK001* mutant is optimal for studying flower development in wheat and could be very important for *Fusarium* head blight resistant projects via conventional crossing.

Introduction

Bread wheat (*Triticum aestivum* L.) is one of the most important staple crops worldwide. The world population continues to grow and arable area is decreasing year by year, therefore higher production in crop plants may prove to be necessary to satisfy the increasing demand for food (FAO, 2015). However, many challenges, inclding biotic and abiotic stresses, severely affect wheat fields and product quality. For instance, *Fusarium* head blight (FHB) is critically damaging wheat security (Walter, Nicholson & Doohan, 2010), and the application of chemical insecticides and fungicides used for controlling pests and diseases is increasing the amounts of residues in wheat and in the environment (Hollingsworth et al., 2008). Therefore, scientists and breeders have to find eco-friendly and cost-effective strategies to guarantee wheat yield and quality. Induced mutation methods, such as Cobalt-60 (^{60}Co-γ-ray)-mutagenesis, static magnetic fields (SMFs)-mutagenesis, spaceflight-mutagenesis, and ethyl methane sulfonate (EMS), are important for crop breeding improvement (Krasileva et al., 2017).

In the last decade, severe epidemics caused by *Fusarium* spp. have occurred worldwide with up to 100% yield loss recorded under optimal disease conditions (Yumurtaci et al., 2017). FHB is a complex disease. The *pore-forming toxin-like* (*PFT*) gene at the quantitative trait locus (QTL) *Fhb1,* which was the first FHB-resistance gene isolated, was found to confer resistance to FHB in Sumai 3 (SM3) (Rawat et al., 2016). FHB infection usually occurs on the inner surfaces of lemmas and paleae after germination of the *Fusarium* spp. conidia (Zange, Kang & Buchenauer, 2005). The anther can provide the initial path for FHB infection (Pugh, Johann & Dickson, 1933; Walter, Nicholson & Doohan, 2010); therefore, cleistogamous cultivars, which contain few anthers exposed to glumes, may provide structural barriers for diseases that appear during the flowering stage. In barley (*Hordeum vulgare* L.), cleistogamous cultivars, which self-fertilize within permanently closed flowers (Culley & Klooster, 2007), showed greater resistance to FHB infection than chasmogamous cultivars, which have open flowers (Yoshida, Kawada & Tohnooka, 2005). In wheat, cleistogamous cultivars (U24) have a lower risk of FHB infection than chasmogamous cultivars such as Saikai 165 (Kubo et al., 2010). Therefore, cleistogamy is a new strategy for controlling *Fusarium* head blight.

Cleistogamy in barley is genetically determined by the presence of the recessive allele *cly1*, but the dominant allele at the linked locus, *Cly2*, is epistatic over *cly1* (Wang et al., 2013). Loss of the miRNA172 target site causes *cly1* to express a protein, HvAP2, which effectively suppresses lodicule swelling (Turuspekov et al., 2004; Nair et al., 2010; Wang et al., 2015). In rice (*Oryza sativa* L.), there are many cleistogamous mutants resulting from abnormal lodicules. A single recessive gene, *lodiculeless spikelet(t)* [*ld(t)*], controls the cleistogamous mutant lacking

lodicules (Won & Koh, 1998; Maeng et al., 2006). Another rice mutant, which has a truncated DEP2 determined by the *cl7(t)* gene, has a cleistogamous phenotype because of weak swelling ability in the lodicules (Ni et al., 2014). A third rice mutant, *spw1-cls*, has normal stamens, but the lodicules are transformed homeotically into lodicule-glume mosaic organs, thereby engendering cleistogamy with temperature-sensitivity (Yoshida et al., 2007; Ohmori et al., 2012). A novel temperature-stable cleistogamous mutant, *spw1-cls2*, can maintain the cleistogamous phenotype under low temperatures (Lombardo et al., 2017). The glumes open in the flowering stage because the swelling of the lodicule is primarily responsible for pushing the lemma and palea, thereby opening the floret (Nair et al., 2010). In contrast, there is very little information on cleistogamy in wheat.

The probability of primary infection is approximately proportional to the number of spores reaching the open florets during the flowering process; accordingly, the breeding of varieties of flower that are partially or completely cleistogamous might reduce *Fusarium* susceptibility in wheat (Schuster & Ellner, 2008). In order to probe the mechanism of cleistogamy, Ning et al. (Ning et al., 2013) studied the structure, transcription and post-transcriptional regulation of the cleistogamous gene, *TaAP2*, which is homologous in barley and wheat. *TaAP2* alleles may also generate a cleistogamous wheat and improve resistance to FHB. Additionally, anther extrusion is a complex trait with significant markers; it has either favourable or unfavorable additive effects and imparts minor to moderate levels of phenotypic variance in spring and winter wheat (Muqaddasi et al., 2017). Okada et al. (Okada et al., 2018) proposed a novel mechanism where ovary swelling could push the lemma and palea apart to open the florets in wheat flowers.

Large-scale transcriptomic analyses have been employed in wheat to better understand the molecular mechanisms of flower development (Winfield et al., 2010; Diallo et al., 2014; Feng et al., 2015; Kumar et al., 2015; Yang et al., 2015; Ma et al., 2017). However, because of post-transcriptional and post-translational modifications, the mRNA levels do not always correlate with the corresponding protein levels (Schweppe et al., 2003; Canovas et al., 2004; Zhao et al., 2013). Proteins are directly correlated with cellular functions (Yan et al., 2005; Zhang et al., 2012); therefore, proteomic analysis is essential for studying global protein expression levels in wheat to further unravel the complex mechanisms of cleistogamy. In particular, isobaric tags for relative and absolute quantitation (iTRAQ) technology, which is a quantitative gel-free proteomic approach, coupled with liquid chromatography-tandem mass spectrometry (LC-MS/MS) enables the direct quantification and comparison of protein levels among samples with more efficiency and accuracy than traditional gel-based techniques which fail to identify low-abundance protein species and have limitations for identifying proteins with extreme biochemical properties (Wu et al., 2006).

Here, we show that an SMFs-induced wheat mutant, *ZK001*, is a cleistogamous line with lower FHB infection vulnerability than the chasmogamous line, Yumai 18 (YM18). Additionally, we performed a comparative proteomic analysis of different development stages in YM18 and *ZK001* at Bangfei Bioscience (Beijing Bangfei Bioscience Co., Ltd. http://www.bangfeibio.com/) to characterise the protein expression profiles. In this manner, we

aim to provide insight into proteomic changes associated with the cleistogamous phenotype in wheat, specifically exploring lodicule expanding mechanisms at the protein level. Our results have the potential to benefit future research efforts in controlling FHB via conventional crossing and to advance the study of wheat flower development. They could also contribute to better control of genetically modified lines of agriculturally important crops and have time-saving and cost-saving benefits for the purification of genotypes.

Materials & Methods

Plant Material

The cleistogamy mutant line, *ZK001*, was isolated from a mutagenised population of wheat varieties, YM18, using an SMFs of 7 Tesla for 5 hours. After mutagenesis, it propagated via self-pollination until the cleistogamous phenotype was completely stable. All wheat seeds were stored at the Hefei Institutes of Physical Science, Chinese Academy of Sciences (CASHIPS), Anhui, P. R. China. SM3, Aikang 58 (AK58), YM18 and *ZK001* were grown in a greenhouse in an experimental field (31°54′ N, 117°10′ E) at CASHIPS. Fertilizer and weed management were similar to methods used in the process for wheat breeding (Li et al., 2014). The spikelets and lodicules of YM18 and *ZK001*, which had three biological replicates, were harvested during the white anther stage (WAS), green anther stage (GAS), yellow anther stage (YAS), and anthesis stage (AS) (Zadoks, Chang & Konzak, 1974; Kirby & Appleyard, 1987; Guo & Schnurbusch, 2015). These samples were collected and frozen in liquid nitrogen and preserved at -80 °C.

Starch and total soluble sugar content

Twenty pairs of lodicules with three biological replications from YM18 and *ZK001* were sampled and snap frozen in liquid nitrogen at the four flower development stages. The samples were ground using Tissuelyser-24 (Shanghai Jingxin Industrial Development Co., Ltd.) for 45 seconds at 50 Hz.

Starch and total soluble sugars were extracted following the instructions included with the Starch Content and Plant Soluble Sugar Content test kits (Nanjing Jiancheng Bioengineering Institute). The starch and total soluble sugars in the supernatant were determined using a UV-VIS Spectrophotometer (Lambda 365, PerkinElmer) with a wave length of 620 nm. The starch and total soluble sugar contents were calculated using the following formulas:

$$C_{starch} = \frac{OD_{sample} - OD_{blank}}{OD_{standard} - OD_{blank}} \times \frac{C_{standard\ 1} \times V_{pretreatment} \times \text{Dilution ratio}}{N_{total\ PL}}$$

$$C_{total\ souble\ sugar} = \frac{OD_{sample} - OD_{blank}}{OD_{standard} - OD_{blank}} \times \frac{C_{standard\ 2} \times \text{Dilution ratio}}{10 \times V_{distilled\ water} \times N_{total\ PL}}$$

Note: PL: pair of lodicules, C_{starch}: the starch content in lodicule ($\mu g \cdot PL^{-1}$), $C_{total\ souble\ sugar}$: the total souble sugar content in lodicule ($\mu g \cdot PL^{-1}$), $C_{standard\ 1}$: standard solution 1 concentration = 200 $\mu g \cdot mL^{-1}$, $C_{standard\ 2}$: standard solution 2 concentration = 100 $\mu g \cdot mL^{-1}$, Dilution ratio = 1, $V_{pretreatment}$: the volume of pretreatment solution = 1.7 mL, $V_{distilled\ water}$: the volume of distilled water used for homogenising = 1 mL, $N_{total\ PL}$: the total number of PL which were sampled = 20.

Observation of spikes and lodicules

Spike images of YM18 and *ZK001* were photographed (Nikon) at the AS. After 90 minutes, the lodicules of YM18 and *ZK001*, which were separated from the central young spikes in triplicate during GAS and cultured on Murashige and Skoog (MS) medium, were observed with an upright fluorescence stereomicroscope (Olympus) and photographed (Olympus).

FHB resistance testing

FHB resistance testing was performed during the flowering stage of SM3, AK58, YM18 and *ZK001* in the greenhouse by spraying the FHB spore F0601 (*Fusarium graminearum* Schw. cv. F0601) in both 2013-2014 and 2014-2015. The inoculum (50 μL at 105 spores per mL) was deposited by spraying both sides of the ears. AK58 and SM3 were used as susceptible and resistant controls, respectively. The diseased spikelet rate was calculated using the following formula:

$$\text{Diseased spikelets rate} = \frac{N_{infected\ spikelet}}{N_{total\ spikelet}} \times 100\%.$$

Note: $N_{infected\ spikelet}$: the number of infected spikelet, $N_{total\ spikelet}$: the number of total spikelet.

Protein extraction and iTRAQ labelling

Total soluble proteins were extracted according to a published procedure (Yang et al., 2013) with slight modifications. Briefly, moderate amounts of the samples were separately frozen using liquid N_2 and ground in -20 °C pre-cooled pestles and mortars with urea extraction buffer containing 150 mM Tris-HCl (pH 7.6), 8 M urea, 0.5% SDS, 1.2% Triton X-100, 20 mM EDTA, 20 mM EGTA, 50 mM NaF, 1% glycerol 2-phosphate, 5 mM DTT, and 0.5% phosphatase inhibitor mixture 2 (Sigma). The mixtures were centrifuged at 10,000 × g for 1 h at 4 °C, then the supernatants were mixed with pre-cooled acetone/methanol and incubated for 1 h at -20 °C. The mixtures were centrifuged at 15,000 × g for 15 min at 4 °C. The pellets were washed twice with cold acetone. Pellets were dried and solubilised in lysis buffer containing 50 mM Tris-HCl (pH 6.8), 8 M urea, 5 mM DTT, 1% SDS, and 10 mM EDTA. Protein concentrations of the samples were estimated using the Bradford method (Bradford, 1976) (Table S1) and the samples were stored at -80 °C for further use. All protein samples were checked via sodium dodecyl sulfate polyacrylamide gel electrophoresis (SDS-PAGE) according to the Schägger protocol (Schägger, 2006). SDS-PAGE gels (Figure S1) were stained with Coomassie Brilliant Blue (CBB) staining solution (Coomassie Blue Fast Staining Solution, Beijing Dingguo Changsheng Biotechnology Co., LTD) (Kang et al., 2002).

After determining the protein concentration, we digested the samples with trypsin (Promega, V5113) and then incubated them for 12-16 h at 37 °C. Approximately 100 µg of peptides of the different samples were labelled with iTRAQ based on the protocol of Unwin et al. (Unwin, Griffiths & Whetton, 2010). The peptides of the different samples were labelled with iTRAQ reagents (isobaric tags 113, 114, 115, 116, 117, 118, 119, and 121 for groups YM18-WAS, *ZK001*-WAS, YM18-GAS, *ZK001*-GAS, YM18-YAS, *ZK001*-YAS, YM18-AS, and *ZK001*-AS, respectively) according to the manufacturer's instructions (Applied Biosystems).

HPLC grading of C_{18} columns at high pH and LC-electrospray ionization-MS/MS analysis

The lyophilised peptide mixture was reconstituted with 100 µL of solution A (2% acetonitrile (ACN) and 20 mM ammonium formate, pH 10). Then, the samples were loaded onto a reverse-phase column [C_{18} column, 1.9 µm (particle size), 150 µm (inner diameter) × 120 mm (length), Thermo Scientific] and eluted using a step linear elution program (Table S2). The samples were collected every 1.5 min and centrifuged at 14,000 × g for 5-90 min. The 60 collected fractions were dried and re-dissolved with 5 µL 0.5% formic acid (FA). The collected fractions were finally combined into 10 pools and centrifuged at 14,000 × g for 10 min.

The reconstituted peptides were analysed with the Q-Exactive HF mass spectrometer (Thermo Fisher Scientific) coupled with a nano high-performance liquid chromatography system (1260 Infinity II, Agilent) using 320 °C temperature conditions (Scheltema et al., 2014). The peptides were loaded onto a C_{18} reversed-phase column [C_{18} column, 3 µm (particle size), 100 µm (inner diameter) × 200 mm (length), Thermo Scientific] and separated on an analytical column (XBridge Peptide BEH 130 C_{18} column, Waters) using mobile phases A (0.1% FA/H_2O) and B (0.08% FA, 80% ACN) (Table S3). The HPLC effluent was directly electrosprayed into the mass spectrometer and analysed based on pre-set parameters (Figure S2).

Data analysis

The raw mass data were processed for peptide identification using Proteome Discoverer 1.4 (ver. 1.4.0.288, Thermo Fisher Scientific) with specific parameters (Table S4) for searching the UniProt Triticum database. A false discovery rate (FDR) of ≤ 0.01 was estimated for protein identification using a target-decoy search strategy (Elias & Gygi, 2007). The mass spectrometry proteomics data have been deposited in the ProteomeXchange Consortium (http://proteomecentral.proteomexchange.org) via the PRIDE partner repository (Vizcaino et al., 2016) with the dataset identifier < PXD010188 >. Increasing and decreasing abundant proteins were determined based on 1.5-fold-changes and peptides spectral matches (PSMs) ≥ 2 (Sharma et al., 2017) between *ZK001*-WAS and YM18-WAS (Group 1), *ZK001*-GAS and YM18-GAS (Group 2), *ZK001*-YAS and YM18-YAS (Group 3), *ZK001*-AS and YM18-AS (Group 4), YM18-WAS and YM18-GAS (Group 5), YM18-WAS and YM18-YAS (Group 6), YM18-WAS and YM18-AS (Group 7), *ZK001*-WAS and *ZK001*-GAS (Group 8), *ZK001*-WAS and *ZK001*-YAS (Group 9), and *ZK001*-WAS and *ZK001*-AS (Group 10).

Protein annotation was conducted by a BLAST search against NCBI and UniProt databases. Protein function was classified based on the following databases: Gene Ontology (http://www.geneontology.org/, GO), and Kyoto Encyclopedia of Genes and Genomes

(http://www.genome.jp/kegg/, KEGG). For analysis of differentially abundant proteins (DAPs), significant GO enrichment and KEGG enrichment were defined as a corrected FDR with a *P*–value less than 0.01 (Benjamini & Hochberg, 1995). Proteins containing at least two peptides spectral matches (PSMs) per protein and fold change ratios ≥ 1.5 or ≤ 0.67 were considered more abundant or less abundant proteins, respectively. In order to validate the DAPs profile, we searched the EnsemblPlants database (http://plants.ensembl.org/index.html) for corresponding DNA sequences. A total of 10 DAPs involved in carbohydrate metabolism and calcium ion binding and transport were selected for qRT-PCR validation.

Quantitative real-time PCR validation

Total RNA was isolated using a Plant RNA kit (Omega, R6827) according to the manufacturer's instructions. The quality of each RNA sample was checked on 1% agarose gels. Measurement of the concentration of RNA samples was performed using the NanoDrop 2000 spectrophotometer bioanalyzer (Thermo Fisher Scientific). cDNAs were synthesised using TransScript One-Step gDNA Removal and cDNA Synthesis SuperMix (Transgen Biotech) according to the manufacturer's protocol. qRT-PCR was used to measure the transcript levels of the proteins of interest. Each experiment was performed in three technical replicates with three biological replicates. Target gene-specific primers (Table S5) were designed using the online software Primer 3 version 0.4.0 (http://bioinfo.ut.ee/primer3-0.4.0/primer3/) (Untergasser et al., 2012). Quantitative reverse transcription polymerase chain reaction (qRT-PCR) was performed according to the manufacturer's instructions for the FastStart Essential DNA Green Master (Roche), run on the Roche LightCycler® 96 Instrument. The *glyceraldehyde-3-phosphate dehydrogenase* gene from *T. aestivum* (*TaGAPDH*, GI: 7579063) served as an internal control and the relative expression of target genes was calculated using the $2^{-\Delta\Delta CT}$ method (Livak & Schmittgen, 2001).

Statistical data analysis

The experimental data values represented the average of the measurements conducted from three independent assays and were expressed as the mean ± standard error of the mean (SEM). The data were further analysed using an ANOVA at a 95% confidence level followed by Duncan's test (SPSS 18.0, IBM, Somers, NY, USA). The level of significance was set at $P \leq 0.05$.

Results

Comparative resistance to *Fusarium* head blight

Since the cleistogamous wheat mutant was isolated, its a low rate of FHB infection compared to chasmogamous varieties has been recognized. Kubo et al. (Kubo et al., 2010) showed that cleistogamous wheat cultivars have a lower FHB infection rate than chasmogamous cultivars. Therefore, we tested the FHB resistance of YM18 and *ZK001*. The results of FHB resistance testing showed that the infection rate in Sumai 3 (SM3) and *ZK001* were 7.03% and 9.39% in 2013-2014 and 8.61% and 17.60% in 2014-2015, respectively (Table 1). Compared to SM3 and *ZK001*, YM18 and Aikang (AK58) were highly susceptible: 35.16% and 38.12% in 2014-2015, respectively. However, the diseased spikelet rates for YM18 and AK58 were 15.20% and 20.41% in 2013-2014, respectively, which was half the rate in 2014-2015 (Table 1). This

indicates that the FHB infection rate is greatly influenced by environmental factors. These results suggest that cleistogamous cultivars have a lower FHB infection rate than chasmogamous cultivars. In addition, this mutant should be capable of generating excellent varieties with the phenotype of cleistogamy via conventional hybridization.

Comparison of flowering in YM18 and *ZK001*

In accordance with previous reports, the exserted anthers increased the incidence of FHB (Sage & De Isturiz, 1974; PARRY, JENKINSON & McLEOD, 1995). Furthermore, the anthers of cleistogamy wheat were detained in glums during the flowering stage. Although the individual lines of YM18 and *ZK001* were grown under the same growth and environmental conditions, the morphological differences were obvious. In YM18, the anthers extruded from the palea and lemma at the AS, whereas no anthers were observed in *ZK001* at all flower development stages (Figure 1A). The morphology of the lodicules of YM18 and *ZK001* was also obviously different. In order to investigate their morphology, we harvested the lodicules of YM18 and *ZK001* at the GAS and cultured them for 90 minutes on MS medium. The width of the YM18 lodicules (Figure 1B) was greater than that of the *ZK001* lodicules (Figure 1C and 1D).

Physiological characteristics of lodicules in YM18 and *ZK001*

To reveal the cause of the lodicules difference between YM18 and *ZK001*, we measured the starch and total soluble sugar contents in the lodicules of YM18 and *ZK001* at the four flower development stages. Lodicule starch (Figure 2A, Table S6) and total soluble sugar (Figure 2B, Table S6) contents showed an overall increase from the WAS to the AS for YM18 and *ZK001*. No significant differences in the starch and soluble sugar contents in the lodicule were observed between YM18 and *ZK001* during the WAS or GAS. Additionally, the starch and total soluble sugar contents in *ZK001* during the YAS significantly decreased 2.40 and 1.75-fold, respectively (both $P<0.05$), compared with those in YM18, detected in one pair of lodicules (Figure 2, Table S6). In contrast, the starch and total soluble sugar contents in *ZK001* during the AS remarkably increased 3.57 and 1.52-fold, respectively (both $P<0.05$), compared with those in YM18, detected in one pair of lodicules (Figure 2, Table S6).

Overview of quantitative proteome analysis

In order to study the protein expression patterns in YM18 and *ZK001*, we examined and quantitatively catalogued the proteomes of YM18 and *ZK001* in the four flower development stages using iTRAQ technology. In this study, 19,422 peptides were matched to 4,497 proteins in the samples (Table S7); in addition, 11,603 unique peptides were found, and 2,172 proteins were identified with more than two unique peptide sequences excluding post-translational modifications. As shown in Figure 3A, more than 99% of the peptides covered proteins within the 36 peptides, and protein quantity decreased as the number of matching peptides increased. In terms of protein mass distribution, good coverage (an average of 10%–18% of total proteins in each protein-mass group) was obtained for proteins > 10 kDa and < 60 kDa (Figure 3B). The length of the identified peptides was between 10 and 13 amino acids at the peak and approximately 93% of the peptide length was within 24 amino acids (Figure 3C). Over 77% of the proteins had > 5% sequence coverage. Additionally, sequence coverage distribution was high

in most of the identified proteins: More than 58% had over > 10% coverage and more than 37% had over 20% coverage (Figure 3D). These results indicate that the identified peptides were sufficient for protein identification.

Cluster analysis of protein expression at four developmental stages

In order to identify more differentially abundant proteins (DAPs), we compared DAPs in YM18 and *ZK001* in the flowering development process, *ZK001*-WAS vs YM18-WAS (Group 1), *ZK001*-GAS vs YM18-GAS (Group 2), *ZK001*-YAS vs YM18-YAS (Group 3), *ZK001*-AS vs YM18-AS (Group 4), YM18-WAS vs YM18-GAS (Group 5), YM18-WAS vs YM18-YAS (Group 6), YM18-WAS vs YM18-AS (Group 7), *ZK001*-WAS vs *ZK001*-GAS (Group 8), *ZK001*-WAS vs *ZK001*-YAS (Group 9), and *ZK001*-WAS vs *ZK001*-AS (Group 10). Increasing abundance and decreasing abundance proteins were determined based on fold-changes (FC) of > 1.5 or < 0.667 for expression difference comparison. For further screening, approximately 16, 47, 2, 0, 11, 124, 105, 15, 298 and 188 DAPs were identified with a corrected *P*–value for GO KEGG enrichment less than 0.01 in groups 1 to 10 (Table 2). A Venn diagram of the DAPs and their overlap in Group 1 and Group 2 showed that two common DAPs were increased-abundance and 1 common DAP was decreased-abundance (Figure S3). Group 3 and Group 4 showed no overlap with Group 1 or Group 2 (Figure S3). Venn diagrams indicated that 6, 10, 32, 206, 57, and 140 DAPs were specific DAPs of Groups 5, 8, 6, 9, 7, and 10, respectively (Figure S3).

Functional classification and subcellular localization of proteins

GO analysis showed that all of the identified proteins in YM18 and *ZK001* were involved in 11 subgroups of MF, 19 subgroups of BP, and 14 subgroups of CC (Figure S4). Significant GO enrichment was employed to analyse the DAPs with a corrected FDR *P*–value less than 0.01 and an FC ratio of more than 1.5. Based on GO annotations and enrichments, the DAPs of Group 1 were enriched in molecular function terms for lipid binding (100%) (Figure 4A) as well as biological process terms for lipid transport (14.06%), lipid localization (14.06%), macromolecule localization (20.31%), organic substance transport (20.31%), single-organism transport (15.63%), and single-organism localization (15.63%) (Figure 4B). GO classification of Group 2 revealed that the DAPs were enriched in the biological process, cellular component, and molecular function (Figure 4C). No protein was enriched in Group 3 or Group 4. The DAPs of Groups 5 to 10 were also classified into biological process (Figure S5A), cellular component (Figure S5B) and molecular function (Figure S5C). DAPs involved in carbohydrate metabolism and transport, calcium ion binding and protein transport, fatty acid biosynthesis were further used in cluster analyses.

Accumulation patterns of DAPs and verification of DAPs of interest

Based on the above analyses, 11 genes which corresponded to DAPs of interest were chosen for qRT-PCR analyses using gene-specific primers (Table S5) to explore the expression profile at the transcription level.

The lodicule morphology showed significant differences between YM18 and *ZK001* (Figure 1). We performed qRT-PCR using the RNA of YM18 and *ZK001* lodicules to study the transcript profiles of the 11 genes corresponding to the selected DAPs (Figure 5). The results of

qRT-PCR indicated that the expression level of the gene *A0A1D6CCI3* (encoding the bidirectional sugar transporter SWEET) was expressed in the lodicules at the WAS and GAS of both YM18 and *ZK001*, with almost no expression at the YAS and AS (Figure 3, Table S7); (Figure 5A). Additionally, the expression level of the gene *A0A1D5WGA3* (encoding a nutrient reservoir-related protein) was extremely down-regulated from the WAS to the GAS in both YM18 and *ZK001* (Figure 5B). Though the relative expression level in *ZK001* was significantly higher than that in YM18 in the GAS ($P<0.001$), the relative expression levels were all less than 0.1 in the GAS, YAS or AS in YM18 or *ZK001* (Figure 5B). Compared with the relative expression levels of the gene encoding beta-amylase A0A1D5RR02 in YM18, the gene in *ZK001* was down-regulated during the WAS ($P<0.001$), GAS ($P<0.05$), YAS ($P<0.05$), and AS ($P<0.05$) (Figure 5C). The relative expression levels of *A0A1D5RR02* were all down-regulated from the WAS to the YAS in YM18 and *ZK001*, but there was no significant difference from the YAS to the AS in YM18 or *ZK001* (both $P>0.05$) (Figure 5C). Additionally, compared with its expression in the lodicules of YM18, P93594 (beta-amylase)-encoding mRNA was all up-regulated ($P<0.001$) in the lodicules of *ZK001*, except that in the YAS (Figure 5D). Interestingly, the mRNA level of sucrose synthase W5B5R3 in *ZK001* indicated up-regulation compared with the levels in YM18 at the GAS, YAS, and AS ($P<0.001$), and down-regulation at the WAS ($P<0.05$) (Figure 5E). The mRNA levels of *A0A1D5SYC3* (a gene encoding cellular glucose homeostasis-related proteins) and *A0A1D5VEI9* (a gene encoding cellular glucose homeostasis-related proteins) showed almost the same expression profile as *W5B5R3*, except for that of *A0A1D5SYC3* in the WAS and that of *A0A1D5VEI9* in the AS (Figures 5E, 5F, and 5G). The relative expression level of *A0A1D5RVB4* (a gene encoding cellular glucose homeostasis-related proteins) and *W5B5R3* were similar (Figure 5E and 5H). Compared with expression levels in YM18, the gene expression of beta-glucosidase activity-related protein A0A077S2F2 in *ZK001* was down-regulated ($P<0.05$) during the WAS and GAS and up-regulated ($P<0.001$) in the AS (Figure 5I).

Calcium ion plays a key role in the development of plants. Therefore, the relative expression of the genes encoding calcium ion binding-related protein A0A1D5TN57 and annexin A0A1D5RRV7 were also evaluated to determine the profile during flower development. Compared with levels in YM18, the relative gene expression levels of A0A1D5TN57 in *ZK001* were up-regulated during the WAS and YAS(Figure 5K), and those of A0A1D5RRV7 were up-regulated during the WAS, YAS and AS (Figure 5J). However, the expression levels of *A0A1D5RRV7* and *A0A1D5TN57* were all down-regulated ($P<0.05$) from the WAS to the GAS in *ZK001* (Figure 5J and 5K).

Discussion

Cleistogamy provides structural barriers for diseases of *Fusarium* head blight

From the physiological point of view, the flowering stage is regarded as the most susceptible period for primary infection of wheat spikes by FHB because of the opening of wheat florets and the extension of anthers (Pugh, Johann & Dickson, 1933; Schroeder & Christensen, 1963; Gilsinger et al., 2005; Schuster & Ellner, 2008). Barley is a plant that self-fertilizes with

permanently closed flowers, but chasmogamous barley varieties are easily infected with *Fusarium* (Yoshida, Kawada & Tohnooka, 2005; Culley & Klooster, 2007). Table 1 shows that the diseased spikelet rate in 2014-2015 was more severe than that in 2013-2014 except in SM3, possibly because of the resistance gene *Fhb1* (Rawat et al., 2016). Compared with YM18, which is a wild-type chasmogamous cultivar, the diseased spikelet rate for *ZK001*, a mutant cleistogamous cultivar, decreased by 38.22% and 50.00% in 2013-2014 and 2014-2015, respectively (Table 1). This indicates that although the diseased spikelet rate is greatly influenced by environmental factors, cleistogamous cultivars that flower partially or completely may have a lower risk of FHB infection than chasmogamous cultivars (Kubo et al., 2010; Wang et al., 2013). Therefore, we further verified the hypothesis that cleistogamous wheat cultivars might have lower *Fusarium* susceptibility. A practical strategy for controlling FHB would be to introduce the cleistogamous function into other varieties that are suitable for production and promotion but sensitive to FHB through hybridization.

Lodicules play an important role in glume opening/closing in wheat

The molecular mechanism for cleistogamy has been intensively studied in rice (Maeng et al., 2006; Yoshida et al., 2007; Ohmori et al., 2012; Ni et al., 2014; Lombardo et al., 2017) and barley (Turuspekov et al., 2004; Hori et al., 2005; Nair et al., 2010; Wang et al., 2013, 2015; Zhang et al., 2016). However, the molecular mechanism for cleistogamy in wheat remains unclear, though it is known that the lodicule is a key factor in glume opening/closing in the monocotyledon. The abnormal lodicules may lack the ability to push the lemma and palea apart during the flowering stage in the cleistogamous mutant *ZK001* (Figure 1). This phenomenon is similar to that occurring in barley (Nair et al., 2010).

Carbohydrates and calcium are the main factors regulating lodicule osmotic pressure

Sucrose is the primary form sugar transported for photosynthetic carbon assimilation (Chen et al., 2012). The *A0A1D6CCI3* gene was expressed in the lodicules of both YM18 and *ZK001* (Figure 5A, Table S8). This indicates that carbohydrates can be transferred normally to the lodicules of both YM18 and *ZK001*. Nevertheless, the starch (Figure 2A, Table S6) and soluble sugar (Figure 2B, Table S6) contents of the YM18 lodicules increased dramatically from the GAS to the YAS. Liu et al. (Liu et al., 2017) suggested that retarded lodicule expansion in *ZS97A* was caused by reduced water accumulation because of retarded accumulation of osmotic regulation substances. In contrast, the lower soluble sugar content in the lodicules of *ZK001* prevented the accumulation of water during the YAS (Figure 2B, Table S6). The lodicule size of YM18 was larger than that of *ZK001* because the starch and soluble sugar contents in the lodicules of *ZK001* decreased from the GAS to the YAS, leading to little water transfer to the lodicules. The lodicules of wheat swell extensively and subsequently contract after rapid autolysis of the tissues (Craig & O'Brien, 1975). Accordingly, the starch and soluble sugar contents in the lodicule of YM18 were lower than those in *ZK001* at the AS (Figure 2A and 2B, Table S6).

Cytosolic calcium is an important secondary messenger in plants and plays important roles in the response to both environmental and internal signals (Poovaiah & Reddy, 1993; Liao,

Zheng & Guo, 2017). Plant annexins are calcium-dependent phospholipid binding proteins with many biological functions; for instance, they participate in calcium ion channel formation, membrane dynamics, plant growth and the stress response (Mortimer et al., 2008; Laohavisit & Davies, 2011). In this study, the relative gene expression levels of annexin (A0A1D5RRV7) and the calcium ion binding-related protein (A0A1D5TN57) in the lodicules of *ZK001* were up-regulated during the WAS compared to those of in the lodicules of YM18 (Figures 5J and 5K). Therefore, we infer that the WAS is a critical period for the lodicules.

An overview of the pathways for proteome metabolic changes in lodicules

Many substances regulate the osmotic pressure of lodicules, such as soluble sugar (Zee & O'Brien, 1971; Wang, Gu & Gao, 1991; Yan et al., 2017), starch (Pissarek, 1971), calcium (Qin, Yang & Zhao, 2005; Chen et al., 2016) and potassium (Heslop-Harrison & Heslop-Harrison, 1996; Chen et al., 2016; Liu et al., 2017). Our findings, together with those of previous studies, provide an overview of the metabolic pathways involving the carbohydrates that regulate the osmotic pressure of the lodicules. As shown in Figure 6, sucrose is transferred into the lodicules from the extra-cellular environment through a bidirectional sugar transporter (A0A1D6CCI3), and is converted into D-fructose-6P by hexokinase (A0A1D5SYC3, A0A1D5RVB4 and A0A1D5VEI9) after being broken down into D-fructose. D-fructose-6P converted to α-D-glucose-1P, which can be converted to D-glucose by β-glucosidase (A0A077S2F2) and synthesised into amylose. The starch formed by amylose can be broken down into D-glucose under the action of β-amylase (A0A1D5RR02 and P93594). UDP-glucose formed from amino sugar and nucleotide sugar can also be converted into D-glucose under the action of β-glucosidase (A0A077S2F2). The accumulation of D-glucose leads to a change in osmotic pressure in the lodicules. Additionally, α-D-glucose-1P can enter the pentose phosphate pathway and the fatty acid biosynthesis pathway through the formation of α-D-glucose-6P and β-D-glucose-6P. Soluble sugar can also enter and exit cells through the bidirectional sugar transporter. Furthermore, annexin (A0A1D5RRV7) can trigger calcium ion influx, increasing the osmotic pressure. Once the osmotic pressure changes, water accumulates in / is excreted from the cells of the lodicules and induces the expansion / shrinkage of the lodicules.

Conclusions

The wheat mutant, *ZK001*, with its atrophied, thin and ineffective lodicules lost the ability to push the lemma and palea apart in the flower development process. Compared with YM18, *ZK001* showed a lower rate of *Fusarium* infection because of the cleistogamous phenotype. Furthemore, we speculate that the thin lodicule of *ZK001* resulted from its lower soluble sugar, calcium ion, and potassium ion contents, which were regulated by carbohydrate metabolic, protein transport, and calcium ion binding-related proteins. Though little is known about the mechanism of cleistogamy in wheat, we propose an overview of the metabolic pathway involving the carbohydrate that regulates the osmotic pressure of the lodicules. This study provides foundations for researchers to explore the mechanism of cleistogamy. Furthermore, it shows that it should be possible to generate cleistogamous wheat via conventional crossing,

which would improve the FHB resistance of wheat and control the pollen-mediated gene flow of genetically modified wheat.

Acknowledgements

We thank Prof. Xiue Wang, College of Agriculture, Nanjing Agricultural University, for providing FHB spore F0601. We thank Mr. Shiliang Li and Ms. Shengqun Zheng for field management. We also thank Mrs. Youwei Wu (graphic designer) for instruction in drawing the Figure 6.

References

Benjamini Y, Hochberg Y. 1995. Controlling the False Discovery Rate - a Practical and Powerful Approach to Multiple Testing. *Journal of the Royal Statistical Society Series B-Methodological* 57:289–300.

Bradford MM. 1976. Rapid and sensitive method for quantitation of microgram quantities of protein utilizing principle of protein-dye binding. *Analytical Biochemistry* 72:248–254. DOI: 10.1006/abio.1976.9999.

Canovas FM, Dumas-Gaudot E, Recorbet G, Jorrin J, Mock HP, Rossignol M. 2004. Plant proteome analysis. *Proteomics* 4:285–298. DOI: 10.1002/pmic.200300602.

Chen Y, Ma J, Miller AJ, Luo B, Wang M, Zhu Z, Ouwerkerk PB. 2016. OsCHX14 is Involved in the K+ Homeostasis in Rice (Oryza sativa) Flowers. *Plant Cell Physiol* 57:1530–1543. DOI: 10.1093/pcp/pcw088.

Chen LQ, Qu XQ, Hou BH, Sosso D, Osorio S, Fernie AR, Frommer WB. 2012. Sucrose Efflux Mediated by SWEET Proteins as a Key Step for Phloem Transport. *Science* 335:207–211. DOI: 10.1126/science.1213351.

Craig S, O'Brien TP. 1975. The Lodicules of Wheat: Pre- and Post-Anthesis. *Australian Journal of Botany* 23:451–458. DOI: 10.1071/BT9750451.

Culley TM, Klooster MR. 2007. The cleistogamous breeding system: A review of its frequency, evolution, and ecology in angiosperms. *Botanical Review* 73:1. DOI: 10.1663/0006-8101(2007)73[1:TCBSAR]2.0.CO;2.

Diallo AO, Agharbaoui Z, Badawi MA, Ali-Benali MA, Moheb A, Houde M, Sarhan F. 2014. Transcriptome analysis of an mvp mutant reveals important changes in global gene expression and a role for methyl jasmonate in vernalization and flowering in wheat. *J Exp Bot* 65:2271–2286. DOI: 10.1093/jxb/eru102.

Elias JE, Gygi SP. 2007. Target-decoy search strategy for increased confidence in large-scale protein identifications by mass spectrometry. *Nat Methods* 4:207–214. DOI: 10.1038/nmeth1019.

FAO. 2015. *FAO statistical pocketbook, World food and agriculture 2015, Rome, Food and Agricultural Organization of the United Nations*.

Feng YL, Wang KT, Ma C, Zhao YY, Yin J. 2015. Virus-induced gene silencing-based functional verification of six genes associated with vernalization in wheat. *Biochem Biophys Res Commun* 458:928–933. DOI: 10.1016/j.bbrc.2015.02.064.

Gilsinger J, Kong L, Shen X, Ohm H. 2005. DNA markers associated with low Fusarium head blight incidence and narrow flower opening in wheat. *Theoretical and Applied Genetics* 110:1218–1225. DOI: 10.1007/s00122-005-1953-4.

517 Guo Z, Schnurbusch T. 2015. Variation of floret fertility in hexaploid wheat revealed by tiller
518 removal. *J Exp Bot* 66:5945–5958. DOI: 10.1093/jxb/erv303.
519 Heslop-Harrison Y, Heslop-Harrison JS. 1996. Lodicule Function and Filament Extension in the
520 Grasses: Potassium Ion Movement and Tissue Specialization. *Annals of Botany* 77:573–
521 582. DOI: 10.1006/anbo.1996.0072.
522 Hollingsworth CR, Motteberg CD, Wiersma J V, Atkinson LM. 2008. Agronomic and Economic
523 Responses of Spring Wheat to Management of Fusarium Head Blight. *Plant Disease*
524 92:1339–1348. DOI: 10.1094/PD1S-92-9-l339.
525 Hori K, Kobayashi T, Sato K, Takeda K. 2005. QTL analysis of Fusarium head blight resistance
526 using a high-density linkage map in barley. *Theor Appl Genet* 111:1661–1672. DOI:
527 10.1007/s00122-005-0102-4.
528 Kang DH, Gho YS, Suh MK, Kang CH. 2002. Highly sensitive and fast protein detection with
529 coomassie brilliant blue in sodium dodecyl sulfate-polyacrylamide gel electrophoresis.
530 *Bulletin of the Korean Chemical Society* 23:1511–1512. DOI:
531 10.5012/bkcs.2002.23.11.1511.
532 Kirby EJM, Appleyard M. 1987. *Cereal Development Guide*. 2nd ed Stoneleigh, UK: NAC
533 Cereal Unit, 85pp.
534 Krasileva K V, Vasquezgross HA, Howell T, Bailey P, Paraiso F, Clissold L, Simmonds J,
535 Ramirezgonzalez RH, Wang X, Borrill P. 2017. Uncovering hidden variation in polyploid
536 wheat. *Proc Natl Acad Sci U S A* 114:E913.
537 Kubo K, Kawada N, Fujita M, Hatta K, Oda S, Nakajima T. 2010. Effect of cleistogamy on
538 Fusarium head blight resistance in wheat. *Breed Sci* 60:405–411. DOI:
539 10.1270/jsbbs.60.405.
540 Kumar RR, Goswami S, Sharma SK, Kala YK, Rai GK, Mishra DC, Grover M, Singh GP,
541 Pathak H, Rai A, Chinnusamy V, Rai RD. 2015. Harnessing Next Generation Sequencing in
542 Climate Change: RNA-Seq Analysis of Heat Stress-Responsive Genes in Wheat (Triticum
543 aestivum L.). *OMICS* 19:632–647. DOI: 10.1089/omi.2015.0097.
544 Laohavisit A, Davies JM. 2011. Annexins. *New Phytologist* 189:40–53. DOI: 10.1111/j.1469-
545 8137.2010.03533.x.
546 Li QY, Qin Z, Jiang YM, Shen CC, Duan ZB, Niu JS. 2014. Screening wheat genotypes for
547 resistance to black point and the effects of diseased kernels on seed germination. *Journal of*
548 *Plant Diseases & Protection* 121:79–88. DOI: 10.1007/BF03356495.
549 Liao C, Zheng Y, Guo Y. 2017. MYB30 transcription factor regulates oxidative and heat stress
550 responses through ANNEXIN‐mediated cytosolic calcium signaling in Arabidopsis. *New*
551 *Phytologist* 216:163. DOI: 10.1111/nph.14679.
552 Liu L, Zou ZS, Qian K, Xia C, He Y, Zeng HL, Zhou X, Riemann M, Yin CX. 2017. Jasmonic
553 acid deficiency leads to scattered floret opening time in cytoplasmic male sterile rice
554 Zhenshan 97A. *Journal of Experimental Botany* 68:4613–4625. DOI: 10.1093/jxb/erx251.
555 Livak KJ, Schmittgen TD. 2001. Analysis of relative gene expression data using real-time
556 quantitative PCR and the 2-ΔΔCT Method. *Methods* 25:402–408. DOI:
557 10.1006/meth.2001.1262.
558 Lombardo F, Kuroki M, Yao SG, Shimizu H, Ikegaya T, Kimizu M, Ohmori S, Akiyama T,
559 Hayashi T, Yamaguchi T, Koike S, Yatou O, Yoshida H. 2017. The superwoman1-
560 cleistogamy 2 mutant is a novel resource for gene containment in rice. *Plant Biotechnology*
561 *Journal* 15:97–106. DOI: 10.1111/pbi.12594.

562 Ma J, Li R, Wang H, Li D, Wang X, Zhang Y, Zhen W, Duan H, Yan G, Li Y. 2017.
563 Transcriptomics Analyses Reveal Wheat Responses to Drought Stress during Reproductive
564 Stages under Field Conditions. *Front Plant Sci* 8:592. DOI: 10.3389/fpls.2017.00592.
565 Maeng JY, Won YJ, Piao R, Cho YI, Jiang W, Chin JH, Koh HJ. 2006. Molecular mapping of a
566 gene "ld(t)" controlling cleistogamy in rice. *Theoretical and Applied Genetics* 112:1429–
567 1433. DOI: 10.1007/s00122-006-0244-z.
568 Mortimer JC, Laohavisit A, Macpherson N, Webb A, Brownlee C, Battey NH, Davies JM. 2008.
569 Annexins: multifunctional components of growth and adaptation. *Journal of Experimental*
570 *Botany* 59:533. DOI: 10.1093/jxb/erm344.
571 Muqaddasi QH, Brassac J, Borner A, Pillen K, Roder MS. 2017. Genetic Architecture of Anther
572 Extrusion in Spring and Winter Wheat. *Front. Plant Sci* 8:754. DOI:
573 10.3389/fpls.2017.00754.
574 Nair SK, Wang N, Turuspekov Y, Pourkheirandish M, Sinsuwongwat S, Chen G, Sameri M,
575 Tagiri A, Honda I, Watanabe Y, Kanamori H, Wicker T, Stein N, Nagamura Y, Matsumoto
576 T, Komatsuda T. 2010. Cleistogamous flowering in barley arises from the suppression of
577 microRNA-guided HvAP2 mRNA cleavage. *Proceedings of the National Academy of*
578 *Sciences of the United States of America* 107:490–495. DOI: 10.1073/pnas.0909097107.
579 Ni DH, Li J, Duan YB, Yang YC, Wei PC, Xu RF, Li CR, Liang DD, Li H, Song FS, Ni JL, Li
580 L, Yang JB. 2014. Identification and utilization of cleistogamy gene cl7(t) in rice (Oryza
581 sativa L.). *J Exp Bot* 65:2107–2117. DOI: 10.1093/jxb/eru074.
582 Ning S, Wang N, Sakuma S, Pourkheirandish M, Wu J, Matsumoto T, Koba T, Komatsuda T.
583 2013. Structure, transcription and post-transcriptional regulation of the bread wheat
584 orthologs of the barley cleistogamy gene Cly1. *Theoretical and Applied Genetics* 126:1273–
585 1283. DOI: 10.1007/s00122-013-2052-6.
586 Ohmori S, Tabuchi H, Yatou O, Yoshida H. 2012. Agronomic traits and gene containment
587 capability of cleistogamous rice lines with the superwoman1-cleistogamy mutation. *Breed*
588 *Sci* 62:124–132. DOI: 10.1270/jsbbs.62.124.
589 Okada T, Jayasinghe J, Nansamba M, Baes M, Warner P, Kouidri A, Correia D, Nguyen V,
590 Whitford R, Baumann U. 2018. Unfertilized ovary pushes wheat flower open for cross-
591 pollination. *Journal of Experimental Botany* 69:399–412. DOI: 10.1093/jxb/erx410.
592 PARRY DW, JENKINSON P, McLEOD L. 1995. Fusarium ear blight (scab) in small grain
593 cereals—a review. *Plant Pathology* 44:207–238. DOI: doi:10.1111/j.1365-
594 3059.1995.tb02773.x.
595 Pissarek HP. 1971. Untersuchungen über Bau und Funktion der Gramineen-Lodiculae. *Beitrage*
596 *Zur Biologie Der Pflanzen* 47:313–370.
597 Poovaiah BW, Reddy ASN. 1993. Calcium and Signal-Transduction in Plants. *Critical Reviews*
598 *in Plant Sciences* 12:185–211. DOI: Doi 10.1080/713608046.
599 Pugh GW, Johann H, Dickson JG. 1933. Factors affecting infection of Wheat heads by
600 Gibberella saubiuetii. *J Agric Res* 46:771–797.
601 Qin Y, Yang J, Zhao J. 2005. Calcium changes and the response to methyl jasmonate in rice
602 lodicules during anthesis. *Protoplasma* 225:103–112. DOI: 10.1007/s00709-005-0086-6.
603 Rawat N, Pumphrey MO, Liu S, Zhang X, Tiwari VK, Ando K, Trick HN, Bockus WW,
604 Akhunov E, Anderson JA, Gill BS. 2016. Wheat Fhb1 encodes a chimeric lectin with
605 agglutinin domains and a pore-forming toxin-like domain conferring resistance to Fusarium
606 head blight. *Nat Genet* 48:1576–1580. DOI: 10.1038/ng.3706.

Sage GCM, De Isturiz MJ. 1974. The inheritance of anther extrusion in two spring wheat varieties. *Theoretical and Applied Genetics* 45:126–133. DOI: 10.1007/bf00291142.
Schägger H. 2006. Tricine-SDS-PAGE. *Nature Protocols* 1:16–22. DOI: 10.1038/nprot.2006.4.
Scheltema RA, Hauschild JP, Lange O, Hornburg D, Denisov E, Damoc E, Kuehn A, Makarov A, Mann M. 2014. The Q Exactive HF, a Benchtop Mass Spectrometer with a Pre-filter, High-performance Quadrupole and an Ultra-high-field Orbitrap Analyzer. *Molecular & Cellular Proteomics* 13:3698–3708. DOI: 10.1074/mcp.M114.043489.
Schroeder HW, Christensen JJ. 1963. Factors affecting resistance of Wheat to scab caused by Gibberella zeae. *Phytopathology* 53:831.
Schuster R, Ellner FM. 2008. Level of Fusarium infection in wheat spikelets related to location and number of inoculated spores. *Mycotoxin Research* 24:80–87. DOI: 10.1007/BF02985285.
Schweppe RE, Haydon CE, Lewis TS, Resing KA, Ahn NG. 2003. The characterization of protein post-translational modifications by mass spectrometry. *Acc Chem Res* 36:453–461. DOI: 10.1021/ar020143l.
Sharma M, Gupta SK, Majumder B, Maurya VK, Deeba F, Alam A, Pandey V. 2017. Salicylic acid mediated growth, physiological and proteomic responses in two wheat varieties under drought stress. *J Proteomics* 163:28–51. DOI: 10.1016/j.jprot.2017.05.011.
Turuspekov Y, Mano Y, Honda I, Kawada N, Watanabe Y, Komatsuda T. 2004. Identification and mapping of cleistogamy genes in barley. *Theoretical and Applied Genetics* 109:480–487. DOI: 10.1007/s00122-004-1673-1.
Untergasser A, Cutcutache I, Koressaar T, Ye J, Faircloth BC, Remm M, Rozen SG. 2012. Primer3--new capabilities and interfaces. *Nucleic Acids Research* 40:e115. DOI: 10.1093/nar/gks596.
Unwin RD, Griffiths JR, Whetton AD. 2010. Simultaneous analysis of relative protein expression levels across multiple samples using iTRAQ isobaric tags with 2D nano LC-MS/MS. *Nature Protocols* 5:1574–1582. DOI: 10.1038/nprot.2010.123.
Vizcaino JA, Csordas A, del-Toro N, Dianes JA, Griss J, Lavidas I, Mayer G, Perez-Riverol Y, Reisinger F, Ternent T, Xu QW, Wang R, Hermjakob H. 2016. 2016 update of the PRIDE database and its related tools. *Nucleic Acids Research* 44:D447–D456. DOI: 10.1093/nar/gkv1145.
Walter S, Nicholson P, Doohan FM. 2010. Action and reaction of host and pathogen during Fusarium head blight disease. *New Phytol* 185:54–66. DOI: 10.1111/j.1469-8137.2009.03041.x.
Wang Z, Gu Y, Gao Y. 1991. Studies on the mechanism of the anthesis of rice III. structure of the lodicule and changes of its contents during flowering. *Acta Agronomica Sinica* 17:96–101.
Wang N, Ning S, Pourkheirandish M, Honda I, Komatsuda T. 2013. An alternative mechanism for cleistogamy in barley. *Theoretical and Applied Genetics* 126:2753–2762. DOI: 10.1007/s00122-013-2169-7.
Wang N, Ning S, Wu J, Tagiri A, Komatsuda T. 2015. An epiallele at cly1 affects the expression of floret closing (cleistogamy) in barley. *Genetics* 199:95–104. DOI: 10.1534/genetics.114.171652.
Winfield MO, Lu C, Wilson ID, Coghill JA, Edwards KJ. 2010. Plant responses to cold: Transcriptome analysis of wheat. *Plant Biotechnol J* 8:749–771. DOI: 10.1111/j.1467-7652.2010.00536.x.

Won YJ, Koh HJ. 1998. Inheritance of cleistogamy and its interrelationship between other agronomic characters in rice. *Korean Journal of Breeding*.

Wu WW, Wang GH, Baek SJ, Shen RF. 2006. Comparative study of three proteomic quantitative methods, DIGE, cICAT, and iTRAQ, using 2D gel- or LC-MALDI TOF/TOF. *Journal of Proteome Research* 5:651–658. DOI: 10.1021/pr050405o.

Yan S, Tang Z, Su W, Sun W. 2005. Proteomic analysis of salt stress-responsive proteins in rice root. *Proteomics* 5:235–244. DOI: 10.1002/pmic.200400853.

Yan H, Zhang B, Zhang Y, Chen X, Xiong H, Matsui T, Tian X. 2017. High Temperature Induced Glume Closure Resulted in Lower Fertility in Hybrid Rice Seed Production. *Front Plant Sci* 7:1960. DOI: 10.3389/fpls.2016.01960.

Yang Z, Guo GY, Zhang MY, Liu CY, Hu Q, Lam H, Cheng H, Xue Y, Li JY, Li N. 2013. Stable Isotope Metabolic Labeling-based Quantitative Phosphoproteomic Analysis of Arabidopsis Mutants Reveals Ethylene-regulated Time-dependent Phosphoproteins and Putative Substrates of Constitutive Triple Response 1 Kinase. *Molecular & Cellular Proteomics* 12:3559–3582. DOI: 10.1074/mcp.M113.031633.

Yang Z, Peng Z, Wei S, Liao M, Yu Y, Jang Z. 2015. Pistillody mutant reveals key insights into stamen and pistil development in wheat (Triticum aestivum L.). *BMC Genomics* 16:211. DOI: 10.1186/s12864-015-1453-0.

Yoshida H, Itoh J, Ohmori S, Miyoshi K, Horigome A, Uchida E, Kimizu M, Matsumura Y, Kusaba M, Satoh H, Nagato Y. 2007. superwoman1-cleistogamy, a hopeful allele for gene containment in GM rice. *Plant Biotechnol J* 5:835–846. DOI: 10.1111/j.1467-7652.2007.00291.x.

Yoshida M, Kawada N, Tohnooka T. 2005. Effect of row type, flowering type and several other spike characters on resistance to Fusarium head blight in barley. *Euphytica* 141:217–227. DOI: 10.1007/s10681-005-7008-8.

Yumurtaci A, Sipahi H, Al-Abdallat A, Jighly A, Baum M. 2017. Construction of new EST-SSRs for Fusarium resistant wheat breeding. *Comput Biol Chem* 68:22–28. DOI: 10.1016/j.compbiolchem.2017.02.003.

Zadoks JC, Chang TT, Konzak CF. 1974. A decimal code for the growth stages of cereals. *Weed Research* 14:415–421.

Zange BJ, Kang Z, Buchenauer H. 2005. Effect of Folicur® on infection process of Fusarium culmorum in wheat spikes / Wirkung von Folicur® auf den Infektionsprozess von Fusarium culmorum in Weizenähren. *Zeitschrift Für Pflanzenkrankheiten Und Pflanzenschutz* 112:52–64.

Zee S, O'Brien T. 1971. The Vascular Tissue of the Lodicules of Wheat. *Australian Journal of Biological Sciences* 24:797–804.

Zhang X, Guo B, Lan G, Li H, Lin S, Ma J, Lv C, Xu R. 2016. A Major QTL, Which Is Co-located with cly1, and Two Minor QTLs Are Associated with Glume Opening Angle in Barley (Hordeum vulgare L.). *Front. Plant Sci* 7:1585. DOI: 10.3389/fpls.2016.01585.

Zhang H, Han B, Wang T, Chen S, Li H, Zhang Y, Dai S. 2012. Mechanisms of plant salt response: insights from proteomics. *J Proteome Res* 11:49–67. DOI: 10.1021/pr200861w.

Zhao Q, Zhang H, Wang T, Chen S, Dai S. 2013. Proteomics-based investigation of salt-responsive mechanisms in plant roots. *J Proteomics* 82:230–253. DOI: 10.1016/j.jprot.2013.01.024.

699

Figure 1

Figure 1. Characteristics of genotypes in the 2 differential individual lines of YM18 and *ZK001*.

Figure 1. Characteristics of genotypes in the 2 differential individual lines of YM18 and *ZK001*. Comparison of the inflorescence details between YM18 and *ZK001* in post-anthesis stage (Bar = 1 cm) (**A**). Lodicules of YM18 (**B**) and *ZK001* (**C**) which were sampled in GAS and cultured on MS media containing graphite were observed after 90 minutes by microscope (Bar = 1 mm). (**D**) Comparison of lodicule width between YM18 and ZK001. The results presented are the means of four independent experiments expressed as the mean ± standard error of the mean (SEM). The data were further analyzed using an ANOVA at a 95% confidence level following Duncan's test (SPSS 18.0, IBM, Somers, NY, USA). The level of significance was set at $P \leq 0.05$ or $P \leq 0.001$.

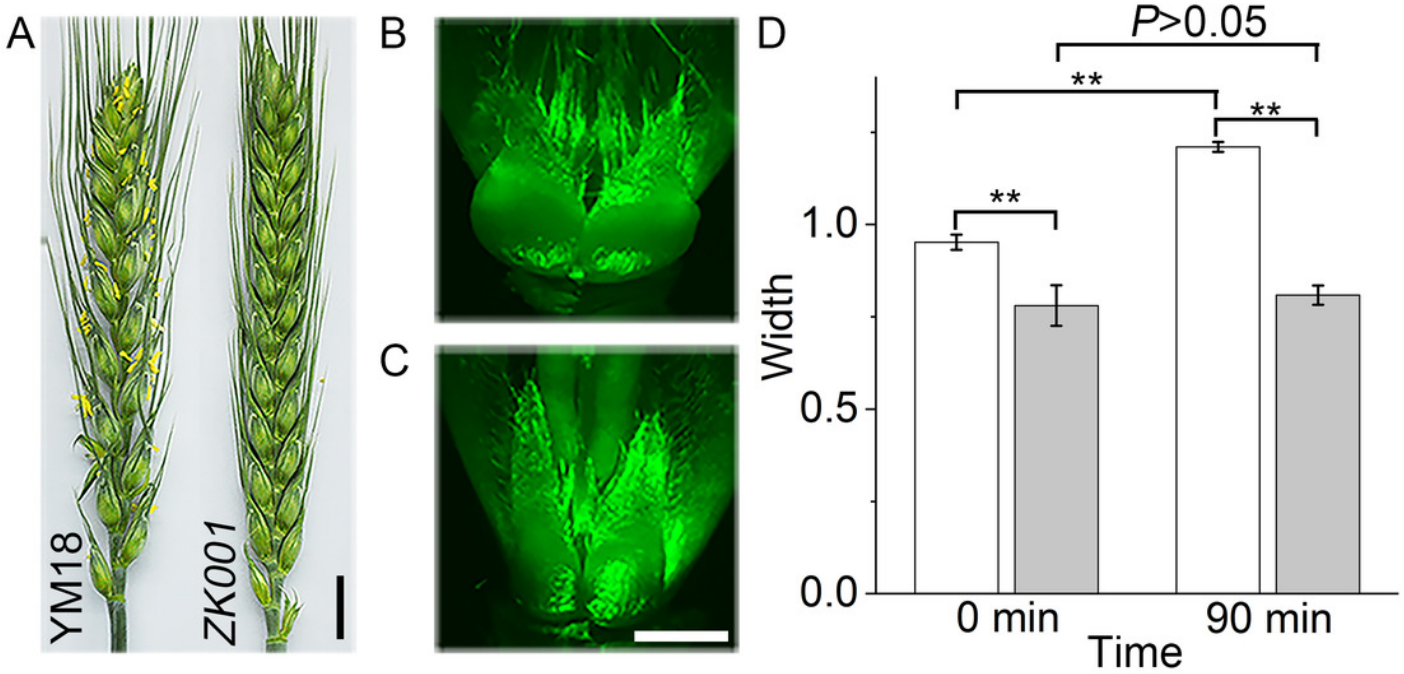

Figure 2

Figure 2. Starch, soluble sugar content in lodicules of YM18 (gray column) and *ZK001* (black column).

Figure 2. Starch, soluble sugar content in lodicules of YM18 (gray column) and *ZK001* (black column). **A:** comparison of starch content change tendency in lodicules between YM18 and *ZK001*. **B:** comparison of soluble sugar content change tendency in lodicules between YM18 and *ZK001*. PL^1: pair of lodicules (PL). The results presented are the means of three independent experiments. Error bars, s.d. Columns marked with different lowercase letter indicate difference in means using the one-way ANOVA LSD analysis of PASW Statistics software among four flower development stage of YM18 (gray lowercase) and *ZK001* (black lowercase). The asterisk indicates the difference between YM18 and *ZK001* at WAS, GAS, YAS and AS, respectively. Duncan tests ($P < 0.05$) were used to detect significant differences between means.

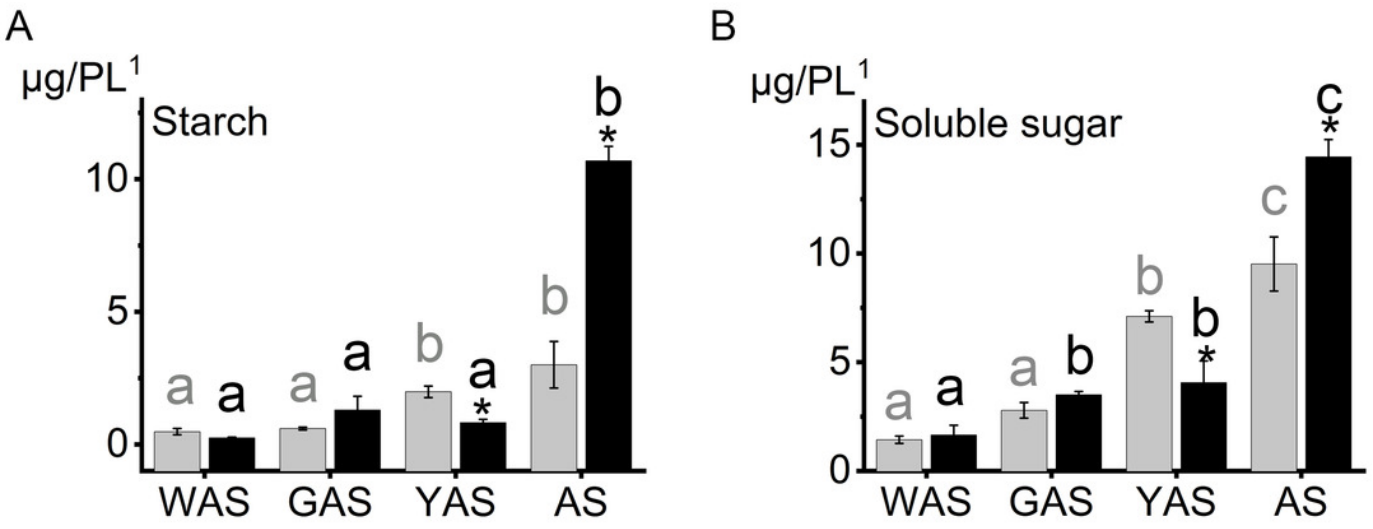

Figure 3

Figure 3. Assessment of iTRAQ analysis for peptides identification and quantitation.

Figure 3. Assessment of iTRAQ analysis for peptides identification and quantitation. **A**: The distribution of the identification peptide segments counts corresponding to the identification of proteins number. **B**: Distribution of protein's molecular weight. **C**: Quantification of peptide-length coverage in the identified proteins. **D**: Coverage of protein mass distribution.

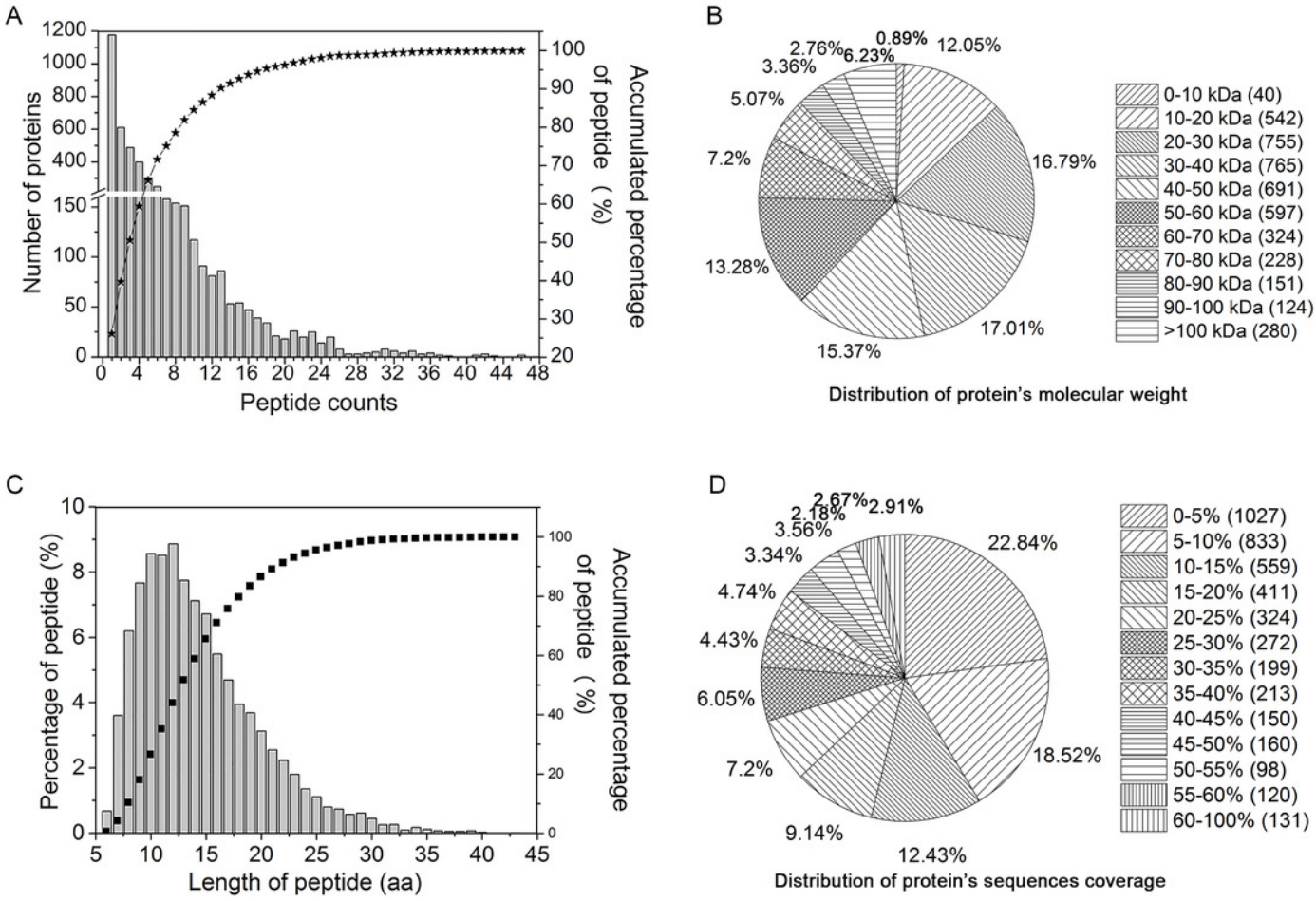

Figure 4

Figure 4. GO classification of DAPs of Group 1 to 4 from four flower development stages in YM18 and *ZK001* based on GO enrichment.

Figure 4. GO classification of DAPs of Group 1 to 4 from four flower development stages in YM18 and *ZK001* based on GO enrichment. **A**: molecular function of Group 1; **B**: biological process of Group 1; **C**: biological process, cellular component and molecular function of Group 2. No protein was enriched in Group 3 or Group 4 basing on GO enrichment. ($0.667 < FC < 1.5$, corrected *P*–value < 0.01, PSMs ≥ 2).

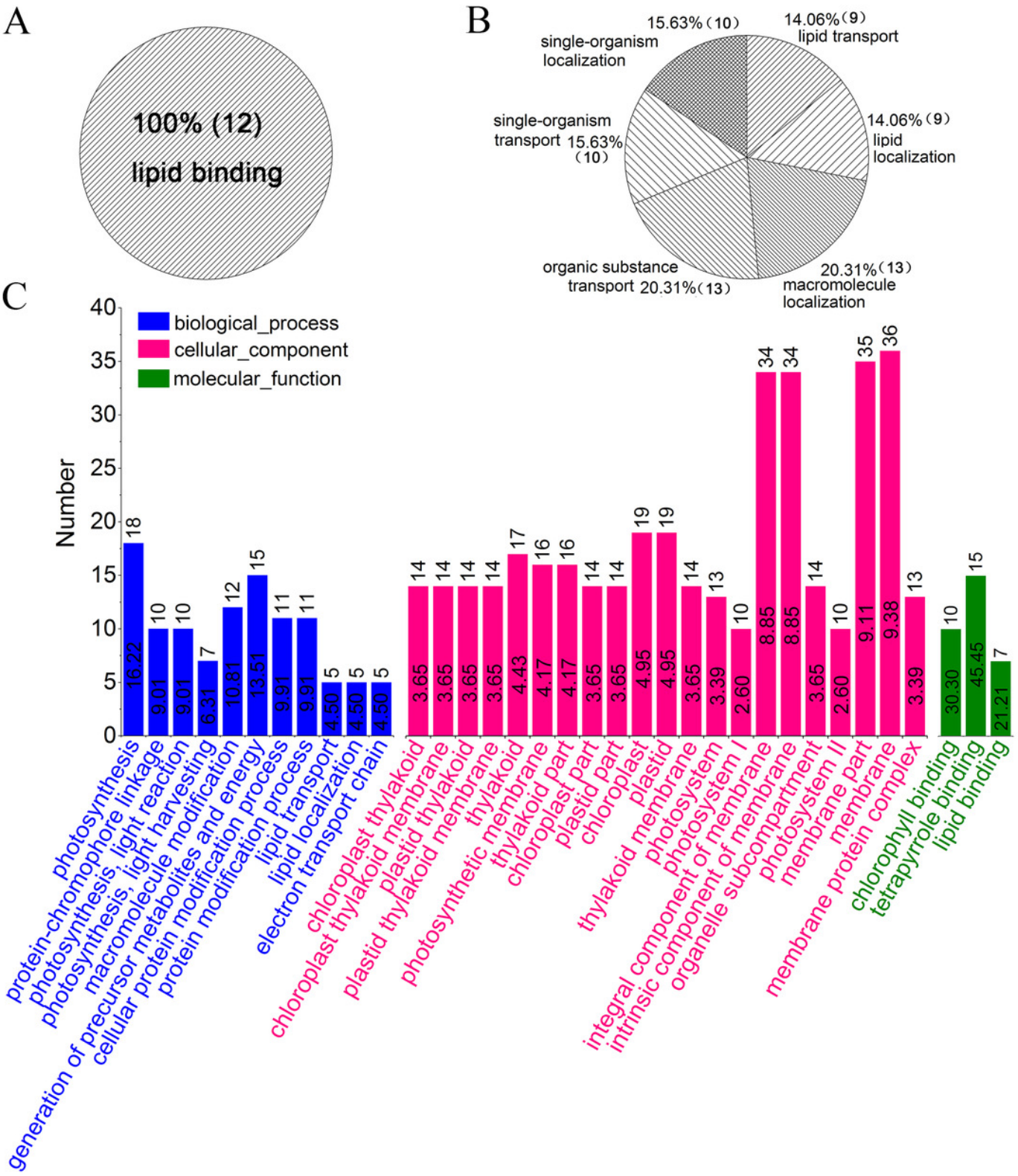
A
100% (12)
lipid binding
B
15.63%（10）
single-organism localization
14.06%（9）
lipid transport
single-organism transport 15.63%（10）
14.06%（9）
lipid localization
organic substance transport 20.31%（13）
20.31%（13）
macromolecule localization
C
biological_process
cellular_component
molecular_function
Number
photosynthesis
protein-chromophore linkage
photosynthesis, light reaction
photosynthesis, light harvesting
generation of precursor metabolites and energy
macromolecule modification
cellular protein modification process
protein modification process
lipid transport
electron transport chain
lipid localization
chloroplast thylakoid
chloroplast thylakoid membrane
plastid thylakoid
plastid thylakoid membrane
photosynthetic membrane
thylakoid
thylakoid membrane
chloroplast part
plastid part
chloroplast
plastid
thylakoid membrane
photosystem
photosystem I
integral component of membrane
intrinsic component of membrane
organelle subcompartment
photosystem II
membrane part
membrane protein complex
membrane
chlorophyll binding
tetrapyrrole binding
lipid binding

Figure 5

Figure 5. Relative expression profile of related genes which corresponded to DAPs in lodicules of YM18 (gray column) and *ZK001* (black column).

Figure 5. Relative expression profile of related genes which corresponded to DAPs in lodicules of YM18 (gray column) and *ZK001* (black column). **A to I:** relative expression profile of carbohydrate-related genes in lodicules of YM18 and *ZK001*. **J to K:** relative expression profile of calcium ion binding-related genes in lodicules of YM18 and *ZK001*. The results presented are the means of three independent experiments. Error bars, s.d. Columns marked with different lowercase letter indicate difference in means of YM18 (gray lowercase) and *ZK001* (black lowercase) using the one-way ANOVA LSD analysis of PASW Statistics software. The asterisk indicates the difference between YM18 and *ZK001* at WAS, GAS, YAS and AS, respectively. Duncan's tests ($P < 0.05$) were used to detect significant differences between means.

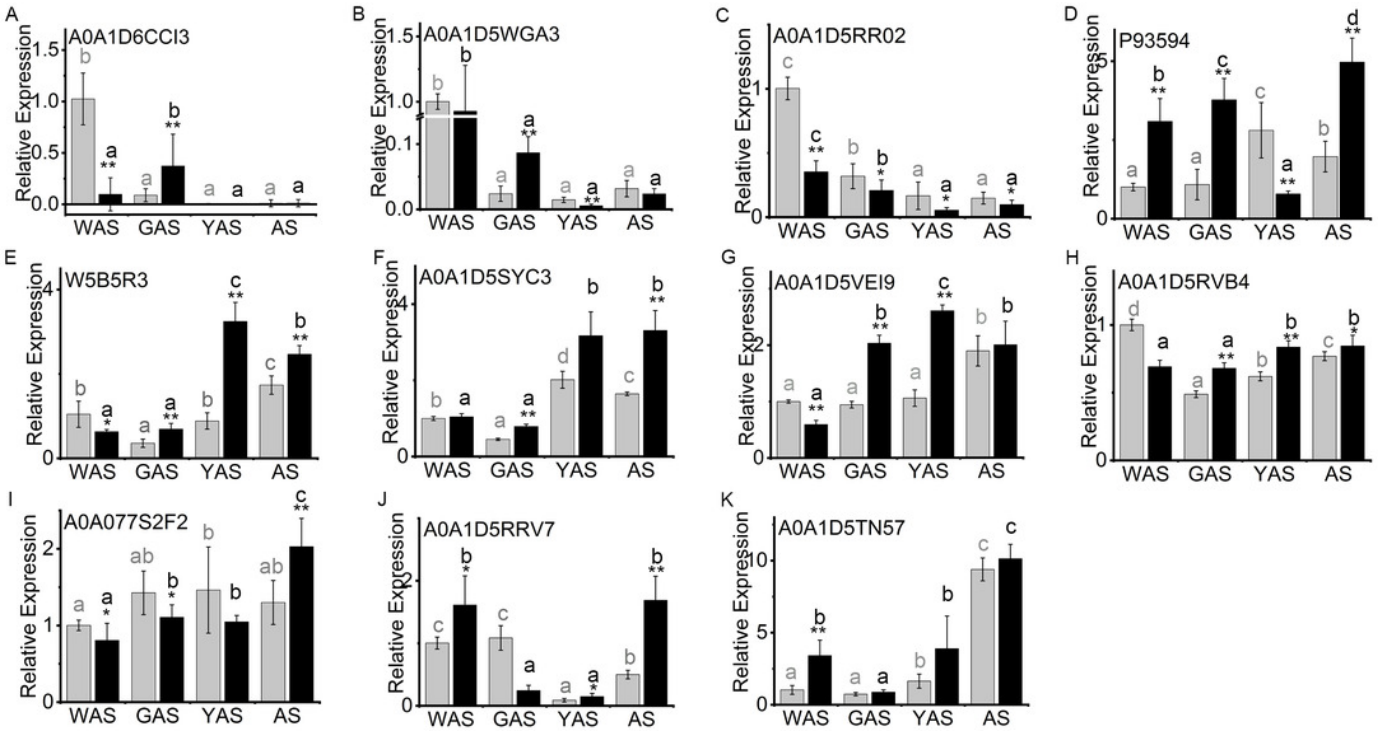

Figure 6

Figure 6. An overview of the pathway for proteome metabolic changes between YM18 and *ZK001*.

Figure 6. An overview of the pathway for proteome metabolic changes between YM18 and *ZK001*. (1) A0A1D6CCI3 (bidirectional sugar transporter SWEET), (2) A0A1D5SYC3 (cellular glucose homeostasis-related proteins), (3) A0A1D5RVB4 (cellular glucose homeostasis-related proteins), (4) A0A1D5VEI9 (cellular glucose homeostasis-related proteins), (5) A0A077S2F2 (beta-glucosidase activity-related protein), (6) W5B5R3 (sucrose synthase), (7) A0A1D5RR02 (beta-amylase), (8) A0A1D5RRV7 (annexin), (9) A0A1D5TN57 (calcium ion binding-related protein), (10) A0A1D5WGA3 (nutrient reservoir-related protein), (11) P93594 (beta-amylase).

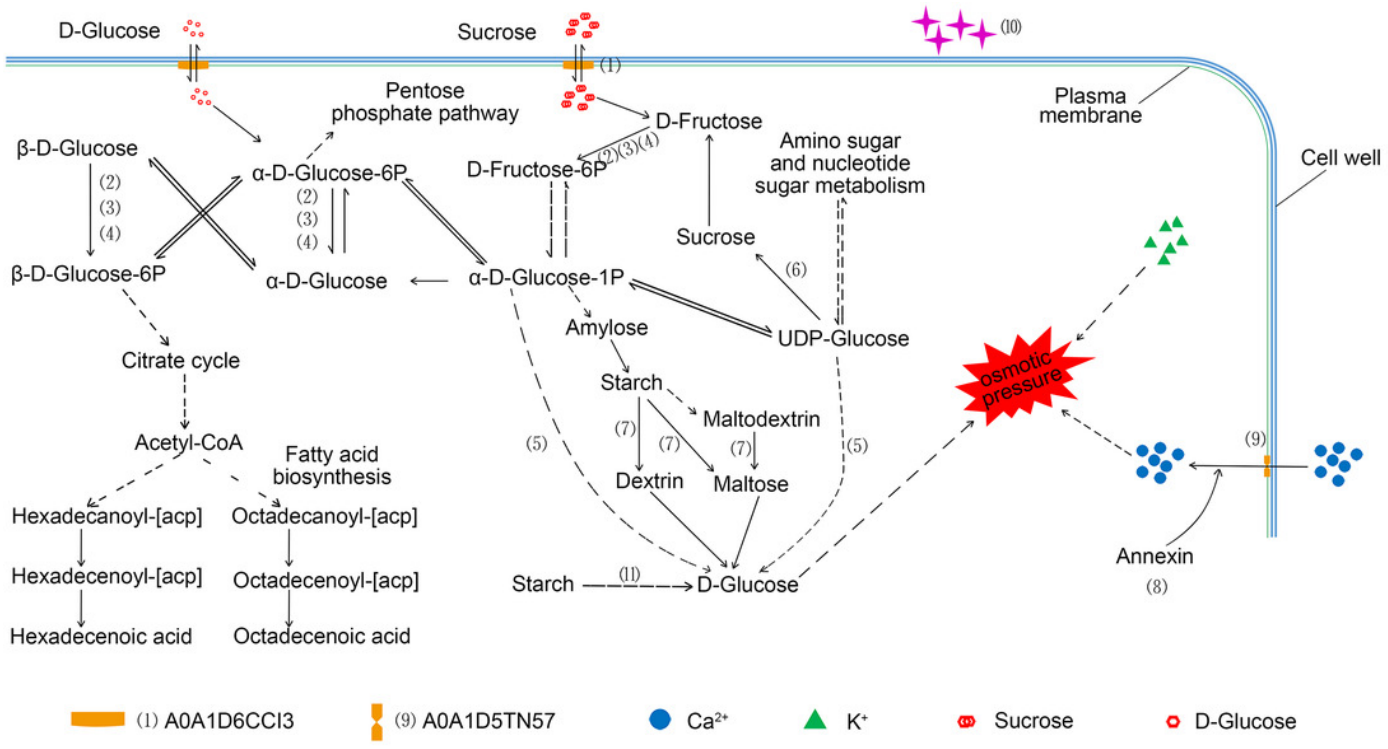

Table 1(on next page)

Table 1. Comparison of diseased spikelets rate by *Fusarium* head blight in 2013-2014 and 2014-2015 in four varieties.

Table 1. Comparison of diseased spikelets rate by *Fusarium* head blight in 2013-2014 and 2014-2015 in four varieties.

Table 1. Comparison of diseased spikelets rate by *Fusarium* head blight in 2013-2014 and 2014-2015 in four varieties.

Variety	Diseased spikelets rate[a] (%)	
	2013-2014	2014-2015
SM3	7.03 ± 2.23	8.61 ± 3.40
ZK001	9.39 ± 3.31	17.60 ± 3.60
YM18	15.20 ± 2.46	35.16 ± 3.71
AK58	20.41 ± 6.76	38.12 ± 6.13

a: Diseased spikelets rate=the number of infected spikelets/total number of spikelets×100%. The results presented are the means of three independent experiments. Error bars, s.d.

Table 2(on next page)

Table 2. The number of differentially abundant proteins (DAPs) at four flower development stages.

Table 2. The number of differentially abundant proteins (DAPs) at four flower development stages. (0.667 < FC < 1.5, corrected *P*–value < 0.01)

Table 2. The number of differentially abundant proteins (DAPs) at four flower development stages. (0.667 < FC < 1.5, corrected *P*–value < 0.01, PSMs ⩾ 2)

Groups	Total	Corrected *P*–value < 0.01		
		Increasing-DAPs	Decreasing-DAPs	Total DAPs
Group 1	4188	7	9	16
Group 2	4188	9	38	47
Group 3	4189	1	1	2
Group 4	4189	0	0	0
Group 5	4188	0	11	11
Group 6	4188	27	97	124
Group 7	4188	31	74	105
Group 8	4188	4	11	15
Group 9	4188	123	175	298
Group 10	4188	94	94	188

Note: Group 1: *ZK001*-WAS vs YM18-WAS, Group 2: *ZK001*-GAS vs YM18-GAS, Group 3: *ZK001*-YAS vs YM18-YAS, Group 4: *ZK001*-AS vs YM18-AS, Group 5: YM18-WAS vs YM18-GAS, Group 6: YM18-WAS vs YM18-YAS, Group 7: YM18-WAS vs YM18-AS, Group 8: *ZK001*-WAS vs *ZK001*-GAS, Group 9: *ZK001*-WAS vs *ZK001*-YAS, and Group 10: *ZK001*-WAS vs *ZK001*-AS.